ChemComm

COMMUNICATION

View Article Online
View Journal | View Issue

Cite this: *Chem. Commun.*, 2022, **58**, 10080

Received 22nd June 2022,
Accepted 10th August 2022

DOI: 10.1039/d2cc03480h

rsc.li/chemcomm

A red-NIR fluorescent probe for rapid and visual detection of acrolein†

Hai Xu, Chen Zhang, Yu-Qing Zhang, Sheng-Nan Suo, Ya-Wen Wang * and Yu Peng *

A novel red-NIR probe (SWJT-8) for detecting acrolein by utilizing the Michael addition reaction was developed. SWJT-8 exhibits a series of unique advantages, such as colorimetric discrimination, high selectivity and the fastest response. And this probe has been successfully applied to the detection of intracellular acrolein.

Acrolein is a highly toxic unsaturated reactive carbonyl substance (RCS), which can be produced by incomplete combustion of matter such as oil, charcoal, wood and plastics.[1] In living organisms, acrolein can be produced endogenously under the oxidative stress of polyamines, lipids, amino acids and other biomolecules.[2] Acrolein is highly reactive and often causes many immune diseases and inflammations.[3] It is also a strong irritating volatile gas, which can come into contact with the human body through various ways such as the digestive tract, respiratory tract, skin and mucous membranes. Inhalation of acrolein can easily cause symptoms such as tearing, eye pain, headaches, dizziness, coughing and breathing difficulties, and is also one of the causes of lung cancer.[4] The acute and chronic poisoning concentrations of acrolein for organisms in freshwater are 68 μg L^{-1} and 21 μg L^{-1}, respectively. The intolerable concentration is 10 mg m^{-3}.[5] Therefore, rapid and visual detection of exogenous or endogenous acrolein is of great significance.

At present, the common method for the determination of acrolein is the Skraup reaction using *m*-aminophenol.[6] In this method, high performance liquid chromatography (HPLC) is used to separate the products, and it is not suitable for high-throughput analysis of a large number of samples. Based on the convenience and rapidity of fluorescence detection, as the first example, Tetsuo Nagano's team carried out two HPLC-free detections of acrolein, using time-resolved luminescence and a two-step solid-phase system, respectively.[7] For better biological detection, a fluorescence assay based on azide/acrolein click reaction was later reported, which has been successfully applied to the imaging of extracellular acrolein released from oxidatively stressed cells.[8] Recently, a thiol group (–SH) was introduced into a fluorescent probe for acrolein detection in food and cells; however, the response time was 1 to 3 h.[9] To the best of our knowledge, there are only four fluorescent probes for the detection of acrolein, which were mentioned above and further summarized in Table S1 (ESI†). Therefore, the development of a NIR fluorescent probe for real-time monitoring of acrolein under mild conditions is still in high demand.

In connection with our continuing work on NIR fluorescent probes,[10] herein we present the design and synthesis of a new red-NIR fluorescent probe **SWJT-8** for acrolein. Notably, **SWJT-8** exhibited fast, high selectivity, colorimetry, and excellent red-NIR response to acrolein. Based on our previous research, [10b, d] we were surprised to find that after the introduction of a methoxy group at the *ortho*-position of the hydroxyl group of the compound **M1** to obtain **M2** (Fig. S1, ESI†), its fluorescence weakened and the fluorescence quantum yield changed from 0.046 to 0.005 in aqueous solution. The change of the fluorescence was attributed to the twisted intramolecular charge transfer (TICT) effect.[11] And based on this change, turn-on fluorescence responses could be achieved. Guided by this rational analysis, the methoxy group was tethered to the hemicyanine skeleton and the cysteamine group was introduced to compound **M2** as a recognition site for acrolein (Fig. 1). The spectral properties of the generated **SWJT-8** in different solvents were then investigated. It exhibited fluorescence in pure organic solvents. But the fluorescence gradually decreased with the increase of water (Fig. S2, ESI†), and in DMSO/PBS buffer (pH = 7.4, 1 : 1, v/v) solution **SWJT-8** has a lower quantum yield (0.006). A relatively high quantum yield (0.024) was obtained after the Michael addition reaction occurred between **SWJT-8** and acrolein to obtain **M3**, which showed that our design was feasible. The synthesis of the designed **M2** and **SWJT-8** is shown in Scheme S1 (ESI†). Their structures were characterized using ^{1}H NMR, ^{13}C NMR, and HRMS or ESI-MS (Fig. S3–S8, ESI†).

Sichuan Engineering Research Center for Biomimetic Synthesis of Natural Drugs, School of Life Science and Engineering, Southwest Jiaotong University, Chengdu 610031, People's Republic of China. E-mail: ywwang@swjtu.edu.cn, pengyu@swjtu.edu.cn.edu.cn

† Electronic supplementary information (ESI) available. See DOI: https://doi.org/10.1039/d2cc03480h

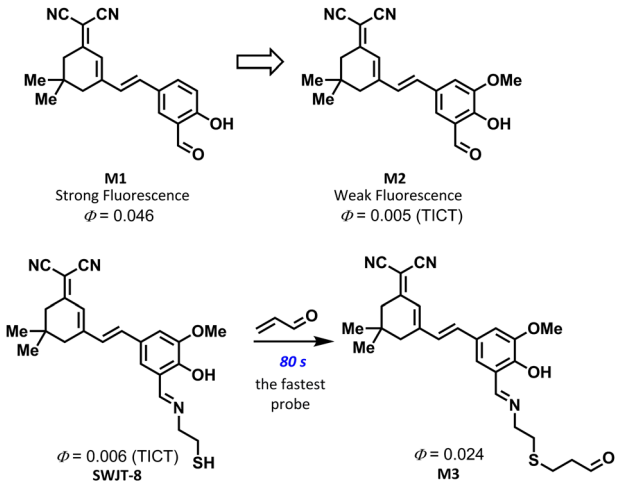

Fig. 1 Design of **SWJT-8** for the detection of acrolein.

First, the pH effect of this probe was investigated. As shown in Fig. S9 (ESI†), its fluorescence intensity was weak in the range of 3.0 to 11.0. After the reaction with acrolein, the fluorescence was significantly enhanced in the range of 6.0 to 9.0. However, considering the application of the probe in biological imaging, 7.4 that is under physiological conditions, was chosen as the best pH value. To verify the feasibility of using **SWJT-8** to detect acrolein, the spectroscopic properties of the probe before and after the addition of acrolein were tested. As shown in Fig. 2, the UV absorption of the probe underwent a large blue shift, and the solution color changed from gray to pink at the same time. When acrolein was added, the fluorescence intensity of the probe was significantly enhanced at 672 nm. These results showed that the probe exhibited good colorimetric and red-NIR detection of acrolein.

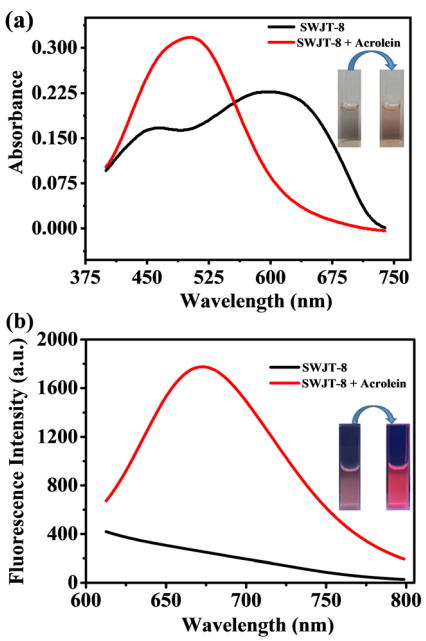

Fig. 2 Absorption spectra (a) and fluorescence spectra (b) changes of 10.0 μM **SWJT-8** to 100.0 μM acrolein in DMSO/PBS buffer (pH = 7.4, 1 : 1, v/v) solution (λ_{ex} = 500 nm). Insets: (a) Under visible light. (b) Under UV light.

The reaction mechanism of **SWJT-8** with acrolein was confirmed using mass spectrometry. The peak at *m*/*z* 464.19 was assigned to $[\mathbf{M3} + H]^+$ (Fig. S10, ESI†). This result was consistent with our speculation and the related literature reports.[7b] At the same time, to better investigate the reaction mechanism of **SWJT-8** with acrolein, ^{1}H NMR titration experiments were performed (Fig. S11, ESI†). With the addition of acrolein to probe **SWJT-8** in DMSO-d_6, the new peaks at 9.64 ppm and 2.80–2.75 ppm were assigned to the aldehyde group $H_{a'}$ and methylene protons, respectively. Notably, the original signal at 5.70 ppm corresponded to the C=N proton H_b of the probe. After the addition of acrolein, it was downfield shifted to 8.45 ppm and the peak of the *o*-hydroxyl group $H_{c'}$ appeared at 13.82 ppm, which indicated that an intramolecular hydrogen bond (C=N···OH) existed. The H-bond will increase the conjugation of the system, which may be the reason for the fluorescence enhancement.[12] In addition, the density functional theory (DFT, Gaussian 09 and B3LYP/6–31G) calculations were used to discuss the correlation between **SWJT-8** and **M3**.[13] As shown in Fig. S12a (ESI†), **SWJT-8** was designed with three rotating rotors, C_{aryl}–C_{vinyl}, O_{alkoxy}–C_{aryl} and C=N, respectively. As shown in Fig. S12b (ESI†), when the dihedral angle of C_{aryl}–C_{vinyl} was 0°, there was a smaller difference in the electron cloud distribution between **SWJT-8** and **M3**. However, when the dihedral angle changed from 0° to 90°, the LUMO electron clouds of **SWJT-8** and **M3** were all distributed on the C≡N moiety. For **SWJT-8**, the HOMO electron clouds were distributed on the benzene ring and the corresponding substituent, which was consistent with the twisted intramolecular charge transfer (TICT) processes (Fig. S12c, ESI†).[14] However, the HOMO electron clouds of **M3** were mainly distributed on the C=N group, which indicated that the extension of the C=N chain could affect the distribution of electron clouds.

Under optimal conditions, the response of **SWJT-8** to acrolein at various concentrations was investigated. As shown in Fig. S13 (ESI†), the absorption peak of 635 nm gradually disappeared; meanwhile the absorption peak of 515 nm gradually increased. As shown in Fig. 3a, the fluorescence intensity of **SWJT-8** at 672 nm increased with the increase of acrolein. In addition, the fluorescence intensity of the probe had a good linear correlation with the concentration of acrolein in the range of 0.5–5.0 μM (Fig. S14, ESI†). The limit of detection (LOD) of **SWJT-8** was calculated to be 0.56 μM,[15] which was lower than the average level (1.4 μM) of acrolein in patients, implying that this probe could be used for the detection of acrolein in biological samples.[16]

Response time is a criterion for the broad applications of probes under mild conditions. The reported probes for acrolein are time-consuming (Table S1, ESI†) and limited in practical applications. The investigation of **SWJT-8** is shown in

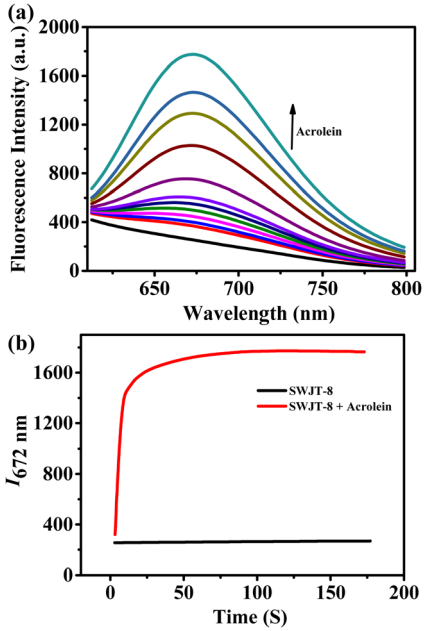

Fig. 3 (a) Fluorescence titration of 10.0 μM **SWJT-8** upon the addition of acrolein (0.0–100.0 μM) in DMSO/PBS buffer (pH = 7.4, 1 : 1, v/v) solution. (b) Response time of 10.0 μM **SWJT-8** towards acrolein at concentrations of 0.0 and 100.0 μM (λ_{ex} = 500 nm).

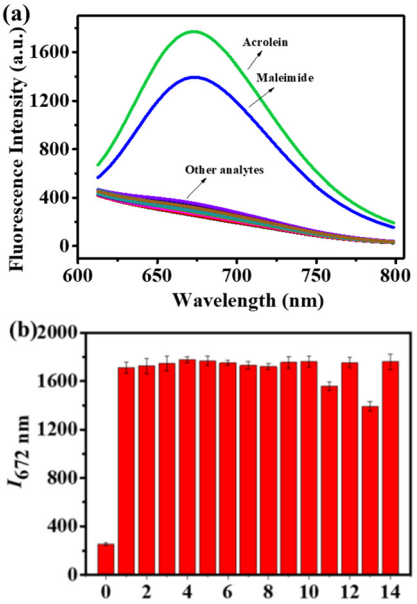

Fig. 4 (a) Fluorescence spectra responses of **SWJT-8** (10.0 μM) to various analytes. (b) Fluorescence response of probe **SWJT-8** (10.0 μM) toward acrolein in the presence of other testing species in PBS/DMSO buffer (pH = 7.4, 1 : 1, v/v) solution [various substances including 100.0 μM (0) blank, (1) formaldehyde, (2) acetaldehyde, (3) glyoxal, (4) acetone aldehyde, (5) *n*-propionaldehyde, (6) pyruvic acid, (7) acetone, (8) allyl alcohol, (9) H_2O_2, (10) OCl^-, (11) Cys, (12) Hcy, (13) maleimide and (14) acrolein] (λ_{ex} = 500 nm).

Fig. 3b, the probe and acrolein reached the reaction equilibrium within only 80 seconds, which was much faster than that of all reported probes currently. And the stability of the probe was good in solution (Fig. S15, ESI†). The above results indicated that **SWJT-8** could achieve rapid detection of acrolein.

In complex biological and environmental samples, a new fluorescent probe is of great significance for the detection of some substance with high selectivity over other substances. Therefore, the selectivity of **SWJT-8** was also examined. As shown in Fig. 4a, the fluorescence intensity of the probe at 672 nm did not change obviously when various aldehydes, allyl alcohol, oxidants, and thiols were added. Only after the addition of acrolein, the fluorescence intensity of the probe was significantly enhanced. Maleimide, a sulfhydryl masking agent, also increased the fluorescence of **SWJT-8**. However, maleimide hardly exists in living cells or the human body, and its interference can thus be ignored.[17] In addition, anti-interference experiments were performed as well. The probe still responded well to acrolein in the presence of other competing interferers (Fig. 4b). Similar results were also observed in the UV spectra. And a blue shift was observed only in the presence of acrolein (Fig. S16a, ESI†). At the same time, the solution color changed significantly from gray to pink only after the addition of acrolein (Fig. S16b, ESI†). The above results showed that **SWJT-8** could specifically be used to identify and detect acrolein by the naked eye.

Encouraged by the rapid response (80 s) and excellent red-NIR properties of **SWJT-8** to acrolein *in vitro*, the feasibility of detecting exogenous and endogenous acrolein using **SWJT-8** was then evaluated (Fig. 5). As shown in Fig. 5a, b, the red channel fluorescence was significantly enhanced after the addition of exogenous acrolein. Hydrogen peroxide (H_2O_2), a reactive oxygen species, enables cells to produce acrolein under oxidative stress.[18] As shown in Fig. 5c, d, after the cells were incubated with hydrogen peroxide at different concentrations, the red channel fluorescence increased with the increase of the hydrogen peroxide concentration. Therefore, **SWJT-8** could be used to detect exogenous and endogenous acrolein in living cells and a tool was provided to evaluate acrolein produced in cells treated with hydrogen peroxide.

In conclusion, a red-infrared fluorescent probe **SWJT-8** for the detection of acrolein was synthesized based on the rational design of substituents on the dicyanoisophorone backbone. This new probe exhibited good colorimetric distinction, high selectivity, and a very fast response (80 s) to acrolein. Furthermore, **SWJT-8** has been successfully applied to image exogenous acrolein and endogenous oxidative stress acrolein in HepG2 cells. Potentially, this work could provide a study tool for further investigating the involvement of acrolein in associated diseases.

This work was supported by the National Natural Science Foundation of China (No. 22071200), and the Fundamental Research Funds for the Central Universities (No. 2682021 ZTPY011) by MoE of China. We also thank Science and Technology Department of Sichuan Province (2020JDRC0021). We would like to thank Analytical and Testing Center of Southwest Jiaotong University for the laser confocal microscope test.

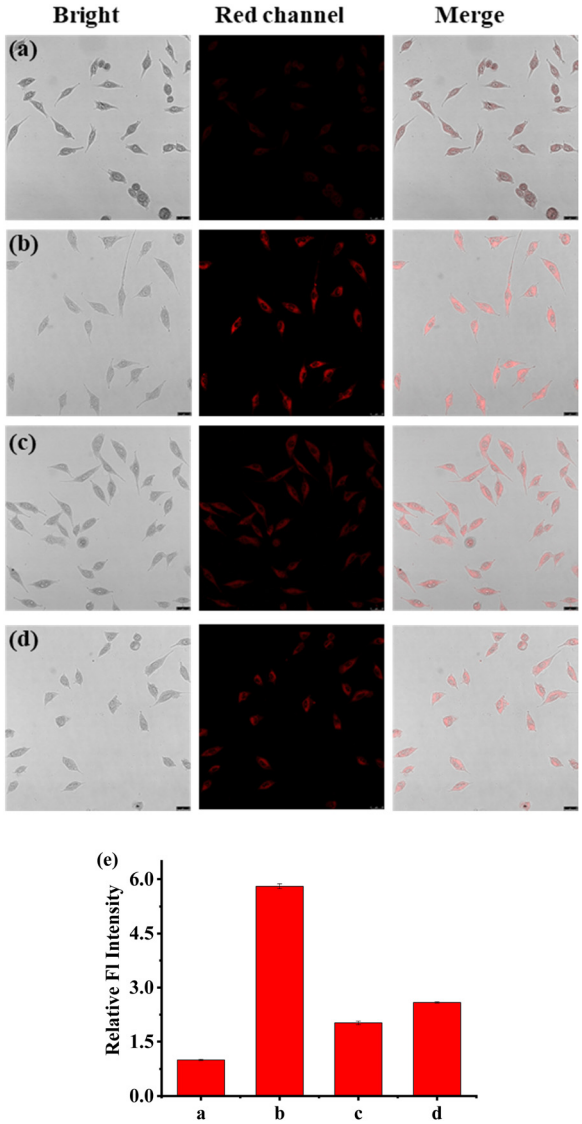

Fig. 5 Confocal fluorescence images of acrolein in HepG2 cells (λ_{ex} = 458 nm). (a) HepG2 cells were incubated with **SWJT-8** (10.0 μM) for 30 min. (b) Cells were pre-incubated with acrolein (100.0 μM) and then with **SWJT-8** (10.0 μM). (c) Cells were pre-incubated with H_2O_2 (200.0 μM) and then with **SWJT-8** (10.0 μM). (d) Cells were pre-incubated with H_2O_2 (500.0 μM) and then with **SWJT-8** (10.0 μM). (e) Relative fluorescence intensity output of groups (a–d).

Conflicts of interest

There are no conflicts to declare.

Notes and references

1 (*a*) K. Hensley, K. A. Robinson, S. P. Gabbita, S. Salsman and R. A. Floyd, *Free Radical Biol. Med.*, 2000, **28**, 1456–1462; (*b*) J. I. Mano, *Plant Physiol. Bioch.*, 2012, **59**, 90–97; M. Singh, A. Kapoor and A. Bhatnagar, *Chem.-Biol. Interact.*, 2015, **234**, 261–273.
2 (*a*) M. K. Mohammad, D. Avila, J. Zhang, S. Barve, G. Arteel, C. McClain and S. Joshi-Barve, *Toxicol. Appl. Pharmacol.*, 2012, **265**, 73–82; (*b*) M. Takamatsu, K. Fukase, R. Oka, S. Kitazume, N. Taniguchi and K. Tanaka, *Sci. Rep.*, 2016, **6**, 1–12.
3 K. Bein and G. D. Leikauf, *Mol. Nutr. Food Res.*, 2011, **55**, 1342–1360.
4 (*a*) Y. Liu, Y. Song, X. Hu, L. Yan and X. Zhu, *J. Cancer*, 2019, **10**, 2788–2799; (*b*) A. Korpi, J. Järnberg and A. L. Pasanen, *Crit. Rev. Toxicol.*, 2009, **39**, 139–193; (*c*) F. Ahmed, S. Hossain, S. Hossain, A. N. M. Fakhruddin, A. T. M. Abdullah, M. A. Z. Chowdhury and S. H. Gan, *SN Appl. Sci.*, 2019, **1**, 1–19.
5 A. V. Krishnan and D. Feldman, *Annu. Rev. Pharmacol. Toxicol.*, 2011, **51**, 311–336.
6 (*a*) M. Kawase, K. Samejima, M. Okada and H. Shibuta, *J. Pharmacobio-Dyn.*, 1979, **2**, 12–18; (*b*) Y. Suzuki and S. Imai, *Anal. Chim. Acta*, 1982, **136**, 155–162; (*c*) F. Bohnenstengel, M. Eichelbaum, E. Golbs and H. K. Kroemer, *J. Chromatogr. B: Biomed. Sci. Appl.*, 1997, **692**, 163–168.
7 (*a*) M. Togashi, Y. Urano, H. Kojima, T. Terai, K. Hanaoka, K. Igarashi, Y. Hirata and T. Nagano, *Org. Lett.*, 2010, **12**, 1704–1707; (*b*) M. Togashi, T. Terai, H. Kojima, K. Hanaoka, K. Igarashi, Y. Hirata, Y. Urano and T. Nagano, *Chem. Commun.*, 2014, **50**, 14946–14948.
8 A. R. Pradipta, M. Taichi, I. Nakase, E. Saigitbatalova, A. Kurbangalieva, S. Kitazume, N. Taniguchi and K. Tanaka, *ACS Sens.*, 2016, **1**, 623–632.
9 K. Jiang, P. Zhou, J. Zheng, C. Huang, J. Hu, H. Guo, J. Ou and S. Ou, *J. Hazard. Mater.*, 2022, **426**, 128118.
10 (*a*) H. Xu, S.-L. Wu, N.-J. Lin, Y. Lu, J. Xiao, Y.-W. Wang and Y. Peng, *Sens. Actuators, B*, 2021, **346**, 130484; (*b*) H. Xu, X.-R. Liu, Z.-H. Cai, J. F. Zheng, Y.-W. Wang and Y. Peng, *Org. Biomol. Chem.*, 2022, **20**, 4782–4786; (*c*) Y.-A. Feng, H. Xu, Y. Zhou, B.-J. Wang, J. Xiao, Y.-W. Wang and Y. Peng, *Sens. Actuators, B*, 2022, **358**, 131505; (*d*) H.-B. Liu, H. Xu, X. Guo, J. Xiao, Z.-H. Cai, Y.-W. Wang and Y. Peng, *Org. Biomol. Chem.*, 2021, **19**, 873–877.
11 (*a*) Y. Erande, S. Kothavale and Nagaiyan Sekar, *J. Solution Chem.*, 2018, **47**, 353–372; (*b*) S. Kothavale and N. Sekar, *Dyes Pigm.*, 2017, **136**, 116–130.
12 S. Erdemir, S. Malkondu and O. Kocyigit, *Microchem. J.*, 2020, **157**, 105075.
13 M. J. Frisch, G. W. Trucks, H. B. Schlegel, G. E. Scuseria, M. A. Robb, J. R. Cheeseman, G. Scalmani, V. Barone, B. Mennucci and G. A. Petersson, *Gaussian 09, Revision A.1*, 2009.
14 S. C. Lee, C. L. Lee, J. Heo, C. U. Jeong, G. H. Lee, S. Kim, W. Yoon, H. Yun, S. O. Park, S. K. Kwak, S. H. Park and O. P. Kwon, *Chem. – Eur. J.*, 2018, **24**, 2888–2897.
15 Y. Shi, F. J. Huo and C. X. Yin, *Sens. Actuators, B*, 2020, **325**, 128793.
16 K. Sakata, K. Kashiwagi, S. Sharmin, S. Ueda and K. Igarashi, *Biochem. Soc. Trans.*, 2003, **31**, 371–374.
17 Y. Kanaoka, M. Machida, K. Ando and T. Sekine, *Biochim. Biophys. Acta, Protein Struct. Mol. Enzymol.*, 1997, **207**, 269–277.
18 (*a*) G. Manda, M. T. Nechifor and T. M. Neagu, *Curr. Chem. Biol.*, 2009, **3**, 22–46; (*b*) C. O'Flaherty and D. Matsushita-Fournier, *Biol. Reprod.*, 2017, **97**, 577–585.